Virchows Arch (1998) 432:461–468

ORIGINAL ARTICLE

Masao Hirasawa · Yasushi Kitaura · Hirofumi Deguchi
Akira Ukimura · Keishiro Kawamura

Spontaneous myocarditis in DBA/2 mice

Light microscopic study with transmission and X-ray analytical electron microscopic studies

Received: 12 September 1997 / 9 December 1997

Abstract DBA/2 inbred mice spontaneously develop myocarditis and a unique form of subepicardial inflammation of the right ventricle characterized by a prominent eosinophilic infiltrate with calcinosis. We studied this myocarditis using light microscopy and both transmission and analytical X-ray electron microscopy, paying particular attention to eosinophil-associated cardiocyte injury. At 5 weeks of age, many eosinophils and mononuclear cells (MNCs) were seen in the subepicardium of the right ventricle. Electron microscopy showed that cardiocytes underwent degenerative changes, including myofibrillar lysis, accumulation of Z-band material and mitochondrial inclusions, and rupture of plasma membranes. The infiltrating eosinophils appeared to be activated, and cells with cytoplasmic vacuoles, suggestive of degranulation, were noted. The myocardial injury was most severe in the 7th week and healed with myocardial fibrosis and calcinosis by the 8th week. Analytical X-ray electron microscopy showed that the calcinosis was initiated in mitochondrial inclusions of injured cardiocytes. The peripheral eosinophil count did not increase during the course of the disease, but there was a positive correlation between the ratio of eosinophils to infiltrated white blood cells (Eo/WBCs) in the right ventricle and the severity of myocardial damage. Eosinophils may play a significant part in subepicardial cardiocyte injury seen in DBA/2 mice.

Key words DBA/2 mice · Myocarditis · Eosinophilic infiltrate · Calcinosis · Cardiocyte injury

Introduction

Myocarditis can be caused by a variety of a etiological agents [4, 5, 13, 14]. Although experimental models using specific strains of inbred mice that develop myocarditis spontaneously exist [7], the incidence and distribution of the disease vary among the strains [6, 7, 24]. In DBA/2 mice, myocarditic disease is usually localized to the epicardium and subepicardium of the right ventricle [1–3, 6, 7, 19, 21, 24, 26, 27].

In a preliminary long-term study using this mouse strain, we found that the epicardial and subepicardial inflammation was characterized by calcinosis and prominent eosinophilic infiltrates [17]. Although cardiac calcinosis has been reported to occur in 90–100% of DBA/2 mice [26], the pathogenesis of this phenomenon remains unknown [27].

Cationic proteins and major basic protein derived from eosinophils are considered to have an injurious effect on cardiocytes in human eosinophilic heart disease [9, 11, 22, 25], but it is unclear whether the eosinophilic infiltrate is important in the pathogenesis of subepicardial inflammation in DBA/2 mice, especially during the acute stage.

In order to clarify this question, we studied the early stages of myocarditis in young DBA/2 mice by light and electron microscopy, paying particular attention to the relationship between infiltrating eosinophils and cardiocyte injury.

Materials and methods

Sixty male 21-day-old DBA/2 mice were obtained from SLC^R (Shizuoka Agricultural Cooperative Association, Shizuoka, Japan). They were fed a standard maintenance diet (3.94 kcal/g, 5.5% fat) and water in a specific pathogen free (SPF) state. They were anaesthetized with an injection of 45 mg/kg pentobarbital sodium i.p. and were killed at 4, 5, 6, 7, 8, and 10 weeks of age. The heart was divided into two blocks, the basal to middle portion of both ventricles for light microscopic study and the right ventricular free wall for electron microscopic study. Blood was collected from each mouse at 5, 6, 7, 8, and 10 weeks by heart puncture and placed in glass tubes containing EDTA for haematological studies.

For light microscopy, heart blocks were fixed in 10% formalin solution and embedded in paraffin. Sections were transversely cut at the midportion of the ventricles and stained with haematoxylin-eosin and Mallory Azan. The percentage of the right ventricle affected by inflammation was determined by a "point-counting" method already described elsewhere [8].

M. Hirasawa (✉) · Y. Kitaura · H. Deguchi · A. Ukimura
K. Kawamura
Third Division of Internal Medicine, Osaka Medical College,
2-7 Daigaku-cho, Takatsuki, Osaka, 569 Japan
Tel.: (+81) 726-83-1221, Fax: (+81) 726-84-6598

For transmission electron microscopy, specimens obtained from the right ventricle were fixed in 3% glutaraldehyde at 4°C for 2 h. After washing in phosphate buffer, the tissue was postfixed in 1% osmium tetroxide, dehydrated in graded alcohols, and embedded in Epon in the lids of Beem capsules. Semi-thin sections were made from the Epon blocks, and ultra-thin sections were then cut consecutively with a diamond knife. The ultra-thin sections were stained with uranyl acetate and lead citrate, and then viewed and photographed with a Hitachi H-800 electron microscope.

Thick sections (1.5–2.0 μm) were prepared in a similar way from Epon blocks, placed on copper grids, and stained with lead citrate for X-ray analytical electron microscopy. The analytical system consisted of a Hitachi H-500 electron microscope equipped with a Kevex 5100 X-ray energy spectrometer system (Kevex, Burlingame, Calif.). The microscope was operated at 75 kV with a beam diameter of approximately 500 Å. X-Rays generated in the specimens by the electron beam were collected with a Kevex 30 mm^2 lithium-drifted silicon detector positioned within 30 mm of the specimen holder tilted at 62° toward the X-ray detector.

The peripheral blood collected in the EDTA tubes was smeared and dried on microscope slides and then stained by the Wright-Giemsa method. The percentage of eosinophils was estimated among the 100 counts of the whole white blood cells using these slides. Blood was diluted with Turk's solution to determine the total number of white blood cells. The total number of eosinophils per cubic millimetre was calculated as the total number of white blood cells × the percentage of eosinophils.

The analytical methods and methods of statistical analyses used were as follows. Between 5 and 10 weeks of age, the eosinophil count (Eo) of each mouse was estimated; the grouped data are expressed as mean±SEM for each stage. For semiquantitative analysis of right ventricular disease, magnified images of the transverse sections of the ventricles were assessed by a "point-counting" method using a simple square lattice. The percentage of the total right ventricle cross-sectional area (Qrv) affected by myocarditis (Qi) was expressed as Qi/Qrv for each animal. Data are reported as mean±SEM for each age group.

Four grades of right ventricular histologic disease were defined:

Grade (0), no apparent change; (+1), minimal change; (+2), moderate change; and (+3), marked change, obtained by group (five investigators) consensus (Fig. 1b). In our semiquantitative analysis of myocardial degenerative changes, myofibrillar lysis and vacuolization were graded (1+) to (4+) based on the severity and the extent of changes as follows: grade (0) no apparent change; (1+) minimal change; (2+) moderate change; (3+) marked change; and (4+) excessively marked change, as defined by Noda [23].

The numbers of infiltrating eosinophils and total white blood cells were determined by light microscopy in tissue sections stained with haematoxylin-eosin and Mallory Azan. Each magnified section was analysed by a computer system (Nikon Microphoto FXA-LUZEX-3, Nikon Corporation) and an electronic image was obtained. The 0.1-mm^2 areas were selected from the computer-generated images. The numbers of local eosinophils and white blood cells (WBCs) and the ratio of Eo to WBCs were obtained for these areas (Fig. 1c). These data are reported as mean ±SEM for each age group, and the Eo/WBC ratios were checked individually to study the correlations with the histological gradings.

The time courses of local eosinophil counts and the peripheral eosinophil counts and the WBC counts, Eo/WBCs ratios, and Qi/Qrv ratios were assessed by one-way analysis of variance and Scheffe's multiple comparison test. Spearman's rank test was used to determine correlations between the ratio of eosinophils to WBCs in the right ventricle and the grades of the various histological findings described above. *P*-values lower than 0.05 were considered statistically significant.

Results

Macroscopically, speckled whitish patches first developed on the surface of the right ventricle in the 5th week, becoming diffuse by the 6th week. These patches were also observed in the lower part of the right atrium. There were no abnormal findings on the surface of the left ventricle. Neither the right nor the left ventricle became dilated during the experiment.

Light microscopically, multiple small necrotic infiltrates of eosinophils and mononuclear cells initially developed in the subepicardium of the right ventricle in the 4th week. By the 5th week, several necrotic foci containing many damaged cardiocytes that contained numerous discrete granules were seen in the epicardium of the right ventricle (Fig. 1a). Numerous eosinophils, lymphocytes, and scattered macrophages were infiltrated within and around the necrotic foci. Eosinophils were occasionally seen adjacent to degenerating cardiocytes. Necrotic foci became more extensive at the 7th week, and were present beneath the epicardium of the right ventricle. By 8 and 10 weeks, the necrotic areas became more fibrotic and heavily calcified, with mildly inflammatory cell infiltrates.

In the peripheral blood, most eosinophils had cytoplasm containing eosinophilic granules, which stained pink-red. Several eosinophils contained many of these cytoplasmic vacuoles.

Approximately 90% of the mice examined during the period of 5–10 weeks after birth (n=51) experienced myocardial disease. Furthermore, 74% of these mice had an associated eosinophilic infiltrate (Table 1). At 7, 8 and 10 weeks of age, 97% of the mice had varying degrees of degenerative and/or inflammatory change of the right ventricular myocardium.

Ultrastructurally, there was mild interstitial oedema of the right ventricular myocardium in 4-week-old mice, and also infiltrates of few mast cells and fibroblasts. By 5 and 6 weeks, macrophages, lymphocytes, and eosinophils were observed migrating from the lumen of capillaries into and around damaged myocardial foci (Fig. 2). Polymorphonuclear leucocytes had also infiltrated these foci. Macrophages and eosinophils were seen adjacent to apparently intact, degenerating, and necrotic cardiocytes.

Table 1 Frequency of clinicopathologic changes in DBA/2 mice from 5 to 10 weeks after birth

Clinicopathologic profile	Frequency in entire group
Myocarditic change and/or myocardial degeneration (diseased mice)	90% (46/51)
Eosinophil infiltration[a]	69% (35/51)
Mononuclear cell (MNC) infiltration[b]	100% (51/51)
Mineralization	67% (34/51)

[a] Equivalent to 74% of diseased mice of 5 to 10 weeks of age

[b] There are some cases without myocardial cell damage despite the presence of a MNC infiltrate

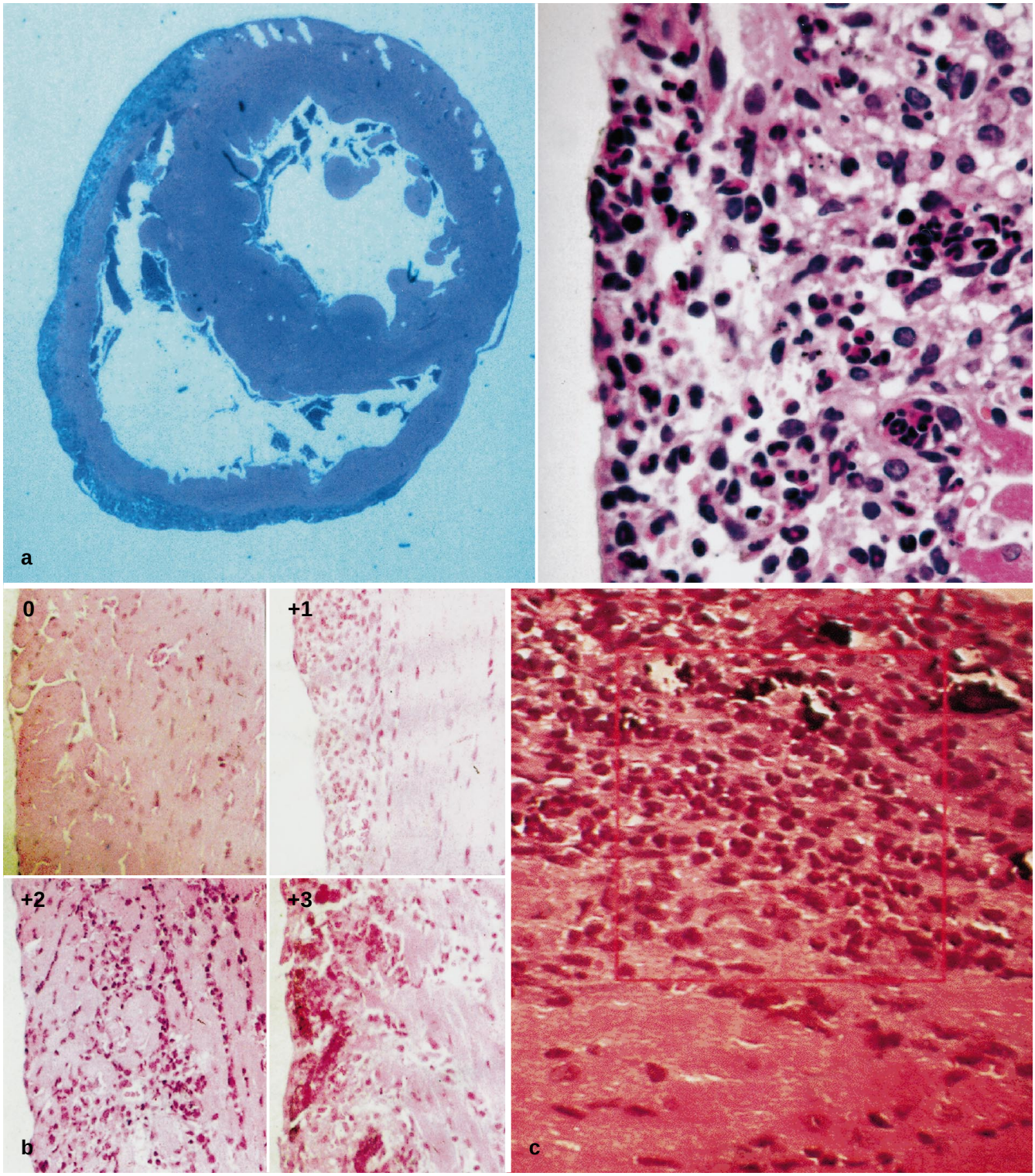

Fig. 1 **a** Transverse section of DBA/2 mouse ventricles at the 5th week. An inflamed area can be found in the subepicardial area of the right ventricular free wall. H&E light micrograph of the inflamed subepicardial area showing myocardial necrosis with cellular infiltration at the 5th week. Numerous mononuclear cells and eosinophils have infiltrated the necrotic area. H&E stain, ×100. **b** Classification of right ventricular histological damage: grade *0* no apparent change, grade *+1* subepicardial inflammation with mild myocardial involvement, grade *+2* subepicardial inflammation with moderate myocardial degeneration, grade *+3* severe subepicardial inflammation and calcinosis with broad and severe myocardial degeneration. **c** Computerized video image of damaged right ventricle. Each frame can be arbitrarily adjusted with the MS-DOS system and is designated as Ai. The 0.1 mm^2 area is obtained as $\sum_{i=1}^{n} Ai\,(A1+A2+A3+.....+An\colon\quad 9 \leqq n \leqq 11)$. The area shown is equal to 0.01 mm^2. The eosinophil and infiltrated white blood cell counts (WBCs) in the Ai frame are then estimated from the photograph shown. Quantification of eosinophils and WBCs was performed by summing the cell numbers calculated per area (A1+A2+.....+An), which corresponds to 0.1 mm^2

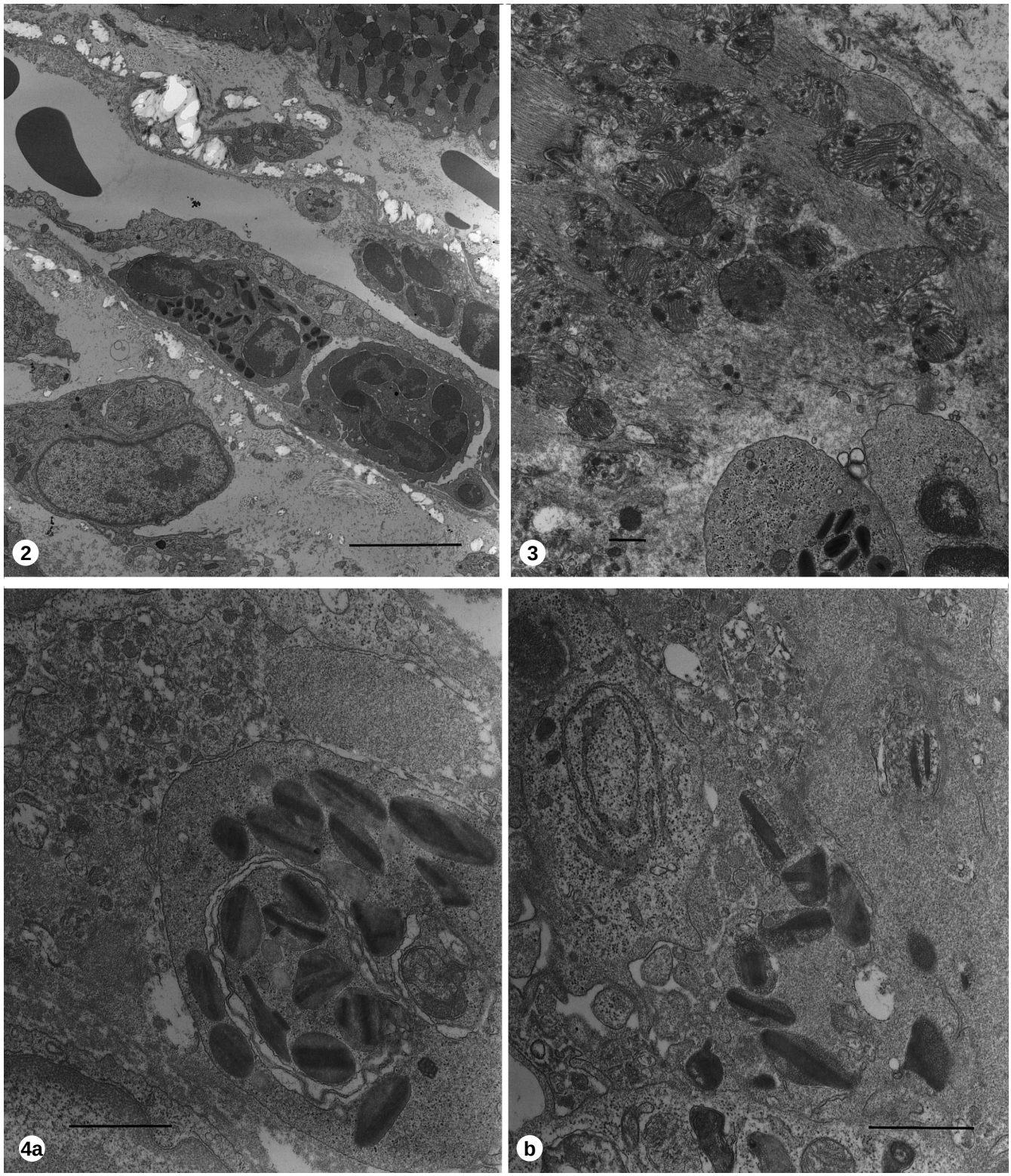

Fig. 2 Electron micrograph of a capillary found in an inflammatory focus. Lymphocytes and eosinophils can be seen between endothelial cells and the basal lamina of the capillary. These cells appear to migrate into the inflammatory focus in the myocardium (5th week). *Bar* 5 μm, ×3,750

Fig. 3 Electron micrograph of a necrotic cardiocyte undergoing myofibrillar lysis. Accumulation of moderately electron-dense mitochondrial inclusions and rupture of the plasma membrane are evident. An eosinophil and a lymphocyte have entered the necrotic cardiocyte (6th week). *Bar* 1 μm, ×6,000

Fig. 4 **a** Electron micrograph of a myocardial necrotic focus (6th week). An eosinophil contains specific granules. **b** Some of these granules have lost their crystalloid internae and display reversed density. The vacuole seen in the cytoplasm of the eosinophil suggests that degranulation has occurred. *Bar* 1 μm, ×16,600

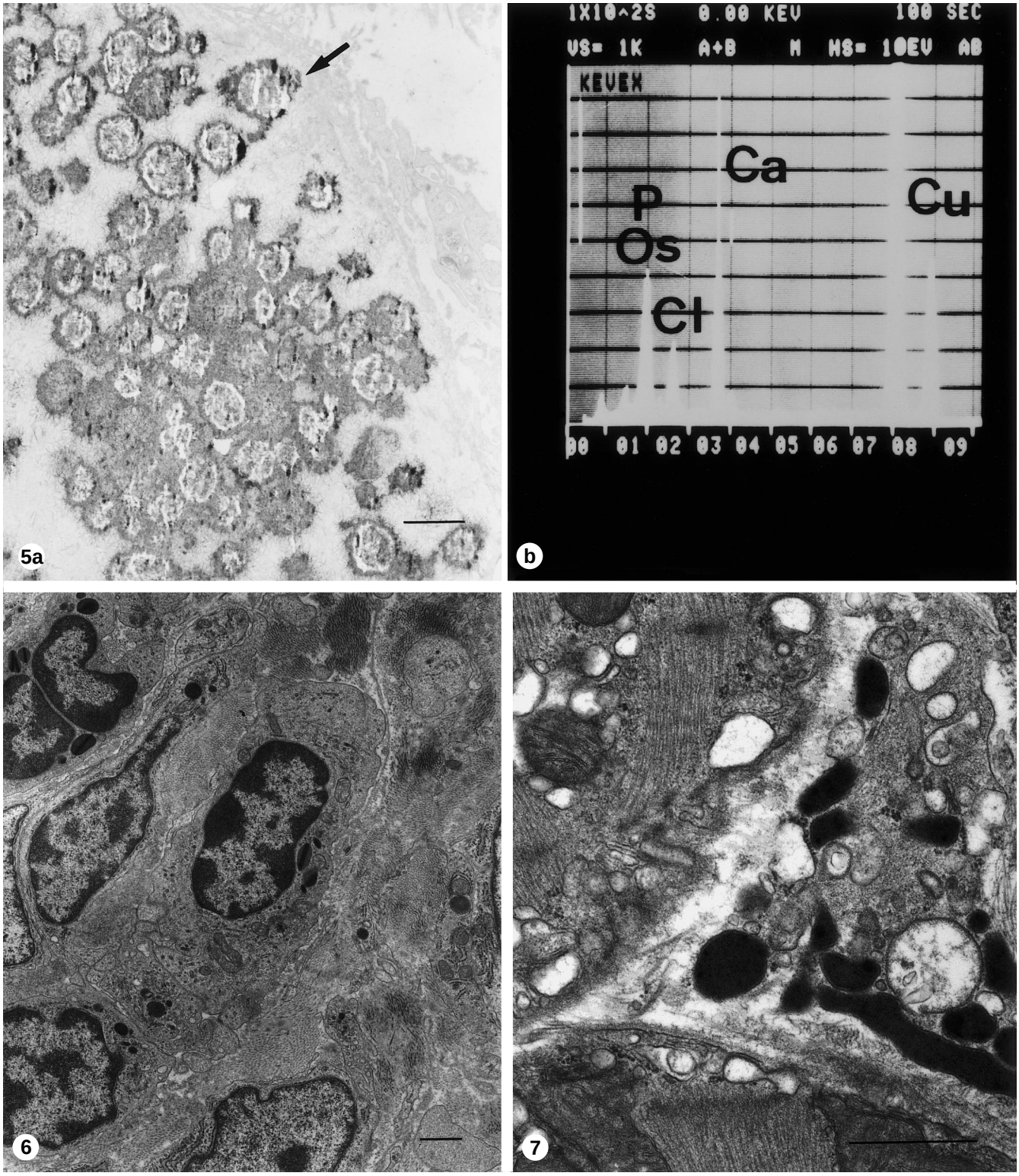

Fig. 5 **a** Electron micrograph of highly electron-dense spicular mitochondrial inclusions in a necrotic cardiocyte during the 6th week. *Bar* 1 μm, ×10,000. **b** Micrograph of summated X-ray spectrum from electron-dense mitochondrial inclusions shown by the arrow in **a**. The significant peak corresponds to calcium (*Ca*: Kα line 3.69 KeV). Prominent peaks for copper (*Cu*) corresponding to the microscope grid, chloride (*Cl*) to the embedding medium, and osmium (*Os*) to the fixing medium are also present

Fig. 6 Electron micrograph of a fibrotic focus present in the myocardium. Numerous collagen fibrils have accumulated in the vicinity of fibroblasts. Eosinophils and lymphocytes can also be seen in the fibrotic area (8th week). *Bar* 1 μm, ×7,200

Fig. 7 Electron micrograph of degenerated cardiocytes in the myocardial fibrotic focus. The cardiocyte has undergone marked degeneration characterized by myofibrillar lysis, accumulation of mitochondrial inclusions and Z-band-like material, and formation of vacuoles (10th week). *Bar* 1 μm, ×22,100

Table 2 Local eosinophil and white blood cell counts (WBCs), Eo/WBCs ratios, and the ratio of inflammatory myocardium to the total right ventricular myocardium (Qi/Qrv) in each subgroup. Also shown is the peripheral blood eosinophil count. Mean±SEM

Age (after birth: weeks)	5 (*n*=11)	6 (*n*=10)	7 (*n*=10)	8 (*n*=10)	10 (*n*=10)
Eosinophil count	50.6±24.6	6.2±2.7	23.7±7.3	17.1±6.7	11.9±6.1
WBC count	196.2±75.9	84.7±32.8	197.5±47.6	173.7±52.7	132.2±37.6
Eo/WBCs ratio (%) (Per 0.1 mm^2 unit in the right ventricular myocardium)	11.5±4.2	5.1±1.6	10.3±2.4	7.2±2.3	5.0±1.8
Qi/Qrv ratio (%)	7.4±4.0	6.0±2.5	10.5±3.5	4.4±1.6	7.8±2.1
Age (after birth: weeks)	5 (*n*=6)	6 (*n*=5)	7 (*n*=5)	8 (*n*=5)	10 (*n*=5)
Eosinophil count (peripheral blood/mm^3)	77.7±12.2	106.4±10.8	142.8±10.3	180.0±20.7	82.0±12.7
		**			**

** $P<0.01$

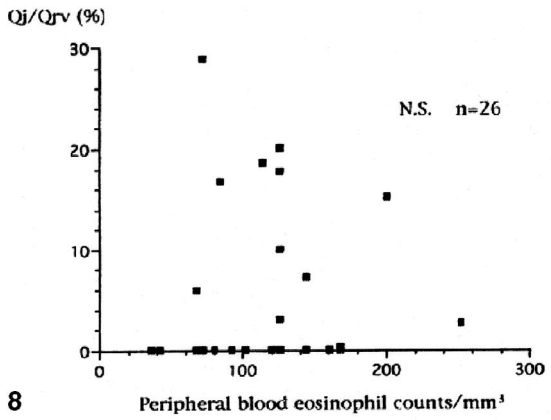

8

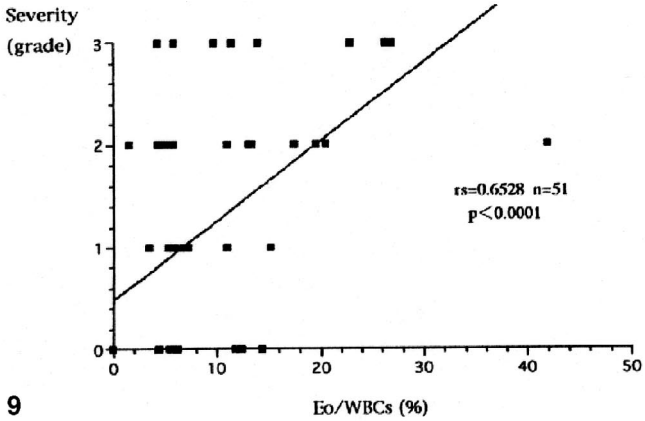

9

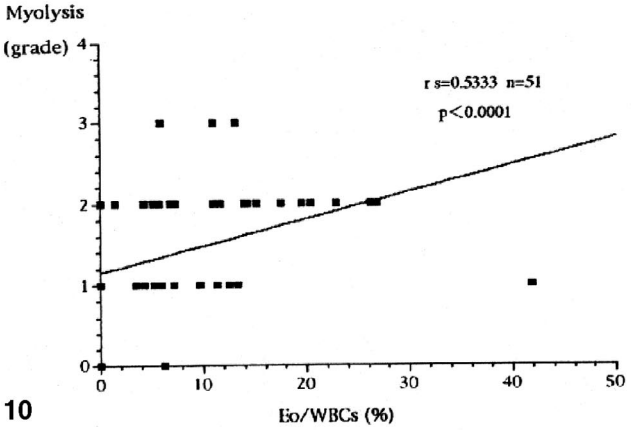

10

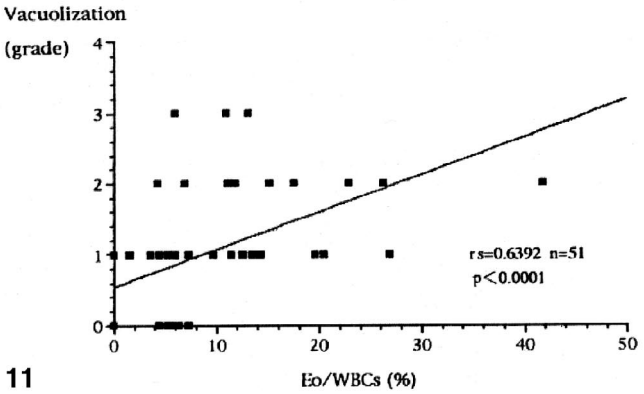

11

Fig. 8 Spearman's rank test was used. Lack of correlation between peripheral blood eosinophil counts and ratio of inflammatory myocardium to total right ventricular myocardium (Qi/Qrv)

Fig. 9 Positive correlation between ratio of eosinophils to white blood cells (*Eo/WBCs*) (per 0.1 mm^2) in the right ventricle and right ventricular histological damage

Fig. 10 Positive correlation between eosinophil/WBCs ratio (per 0.1 mm^2) in the right ventricle and semiquantitative analysis of myolysis

Fig. 11 Positive correlation between eosinophil/WBCs ratio (per 0.1 mm^2) in the right ventricle and semiquantitative analysis of vacuolization

Eosinophils often invaded the necrotic cardiocytes (Fig. 3). These eosinophils that were adjacent to degenerating or necrotic cardiocytes often contained a reduced number of granules, which had lost their normal crystalloid pattern and stained homogeneously (Fig. 4). Cardiocytes found in the inflammatory foci often showed necrosis characterized by myofibrillar lysis and disruption of the plasma membrane at multiple sites. Mitochondria were markedly swollen and frequently contained moderately electron-dense amorphous and/or highly electron-dense spicular inclusions (Fig. 5a). Analytical electron microscopy revealed a prominent peak that corresponded to calcium in the highly electron-dense spicular mito-

chondrial inclusions (Fig. 5b). No calcium peak was identified in the moderately electron-dense amorphous inclusions. After the necrotic cardiocytes had completely broken down, large numbers of calcified mitochondria coalesced to form a large calcified aggregate in the interstitial space. At 8 and 10 weeks, fibroblasts and abundant collagen fibrils were observed in the interstitial space (Fig. 6). Although inflammatory cell infiltrates were less prominent than at 6 and 7 weeks of age, there were still significant numbers of lymphocytes, macrophages, and eosinophils in the interstitial space. Degenerating cardiocytes displayed normal degenerative changes, including myofibrillar lysis, accumulation of myelin figures and formation of vacuoles. Several cardiocytes had undergone necrosis (Fig. 7).

The eosinophil and white blood cell counts (WBCs) in the right ventricle were followed during the period from 5 to 10 weeks after birth (n=51). The eosinophil count was conspicuously high at 5 weeks, but decreased at 7 weeks of age. The WBC count did not change between 5 and 10 weeks of age (Table 2).

For the percentages of the myocardium involved by inflammatory areas (n=51) the 7-week-old mice showed the greatest involvement although there were no significant differences among the subgroups (Table 2). There was no significant correlation between peripheral blood eosinophil counts and the ratio of the inflamed to the total area (Fig. 8).

Peripheral blood eosinophil counts (n=26) revealed that the number of eosinophils was increased in the 8th week compared with other stages ($P < 0.01$) (Table 2).

The correlation between the local eosinophil to WBCs ratio (Eo/WBCs) and the severity of right ventricular histological findings (grades 0,+1,+2,+3) (Fig. 9) was expressed as:

y=0.078x+0.486 rs=0.6528 $P < 0.0001$ n=51

There were also significant relationships between the local eosinophil Eo/WBCs ratio and semiquantification (grades 0,+1,+2,+3,+4) of the myocardial changes (Figs. 10, 11) for the following histological features:

Myofibrillar lysis:

y=0.033x+1.152 rs=0.5333 $P < 0.0001$ n=51

Vacuolization:

y=0.053x+0.545 rs=0.6392 $p < 0.0001$ n=51

Discussion

Viral [4, 5, 17, 18, 20] and/or autoimmune myocarditis [13] typically produce acute myocarditis. In contrast, eosinophilic myocarditis is a chronic disease associated with prolonged eosinophilia, and in particular, with a hypereosinophilic syndrome [22]. However, there are few animal models of idiopathic eosinophilic myocarditis.

DBA/2 strains of inbred mice spontaneously develop epicardial and subepicardial inflammation of the right ventricle. Previous reports have described epicardial and subepicardial damage with myocardial necrosis and interstitial cellular infiltrates in these mice at 4–5 weeks of age [19, 24], as well as residual calcification. In 1984, we first suggested that the epicardial and subepicardial inflammation seen in this mouse strain is characterized by calcinosis and prominent eosinophilic infiltrates on long-term follow-up [16]. The changes are most severe by the 6th and 7th weeks, resolving spontaneously with myocardial fibrosis and calcinosis after the 10th week [16].

We investigated cardiocyte injury during the early stages of this disease within the first 10 weeks of life in the present study. We occasionally found eosinophils in close contact with injured cardiocytes, and eosinophils often invaded necrotic cardiocytes through their ruptured plasma membranes. The infiltrating eosinophils usually contained granules with reversed density, which is characteristic of activated eosinophils [22, 25]. These eosinophils also contained many cytoplasmic vacuoles, which indicates that degranulation had occurred. These phenomena are thought to be similar to the cellular damage seen in the hypereosinophilic syndrome, where cardiocyte injury has been attributed to cationic proteins (ECPs) and major basic proteins (MBPs) derived from granules of activated eosinophils [9, 11, 12]. In the DBA/2 mouse strain, cardiocyte plasma membranes may also be damaged by ECPs and MBPs, resulting in an influx of calcium and necrosis.

From a statistical viewpoint, eosinophil counts in the right ventricular tissue and the Eo/WBCs ratios were highest at 5 weeks and the histological findings were most severe immediately after this period. Only later did peripheral blood eosinophil counts reach a peak (Table 2).

The clinical diagnosis of this disease is often suspected when there is increasing eosinophilia. In our mouse model, the inflammation of the myocardial tissue was widespread before eosinophilia was perceived. Nakayama et al. [22] first suggested, in their clinical study of endomyocardial biopsies, that local deposition of eosinophil-derived proteins was more important in the cardiac myocyte damage than the accumulation of serum proteins. In fact, in the DBA/2 mouse strain, few vacuolated eosinophils were seen in peripheral blood, and peripheral blood eosinophil counts did not correlate with the severity of disease (Fig. 8). Semiquantitative analysis did reveal that the degree of histological myocardial injury correlated positively with the ratio of local eosinophils to white blood cells (Figs. 9–11). These findings also support the impression that local infiltrating eosinophils play a significant role in the cardiocyte injury found in this subepicardial inflammation and myocarditis.

Calcinosis in the injured myocardium is another characteristic feature of this experimental model. The phenomenon has been studied by many investigators at light microscopic level; Van-Vleet and Ferrans [26] were the first to describe mineral deposits in necrotic cardiocytes of DBA/2 mice observed by electron microscopy. They reported that minerals seen in necrotic myocytes formed dense granular and spicular deposits in mitochondria only, mitochondria and the adjacent sarcoplasm, or the entire sarcoplasm.

Our electron microscopic study showed that the calcification appeared to originate in electron-dense inclusions in the mitochondria of necrotic cardiocytes. X-ray analytical electron microscopy demonstrated that the inclusions contained calcium. After the necrotic cardiocytes became organized, multiple calcified lesions coalesced in the interstitial space to form aggregates that persisted as large, dense calcium deposits. These findings are consistent with those described by Van-Vleet and Ferrans [26]. Furthermore, the pathogenesis of the dystrophic calcification characteristic of this model is similar to that of the murine coxsackie B3 myocarditis [4] and EMC viral myocarditis [15, 20]. Deguchi reviewed his findings on X-ray analysis in viral myocarditis and concluded that electron-dense granular or spicular inclusions often appear to increase until the entire mitochondria is occupied by calcium apatite. These calcified granules then would form a larger mass [4].

Our ultrastructural study revealed that mitochondrial calcium accumulation in the postnecrotic areas was much more prominent than that seen in murine coxsackie B3 viral myocarditis.

In conclusion, direct contact between activated eosinophils and cardiocytes was frequently seen in the right ventricular myocardium, suggesting the importance of an immediate response of eosinophilic cationic proteins and/or major basic proteins. The pathogenesis of subepicardial inflammation remains unknown, but the frequency and severity of this disease varies with age [24], gender [24, 27], strain [10], diet [1, 10], genetic susceptibility [2], and hormonal effects [3, 7]. The clinicopathological features of the disease are not identical to those of human hypereosinophilic syndrome.

Overall, the DBA/2 mouse model of myocarditis is very useful for studying the mechanisms of cardiocyte injury mediated by infiltrating eosinophils, especially during the early stages of disease.

Acknowledgements This study was supported in part by a grant-in-aid for scientific research from the Ministry of Education, Science and Culture of the Japanese Government. The authors wish to thank Mrs. A. Saito and Mrs. C. Ota for technical assistance.

References

1. Ball CR, Williams WL (1965) Spontaneous and dietary-induced cardiovascular lesions in DBA mice. Anat Rec 152: 199–210
2. Brownstein DG (1983) Genetics of dystrophic epicardial mineralization in DBA/2 mice. Lab Anim Sci 33:247–248
3. Brunnert SR, Altman NH (1990) Dystrophic cardiac calcinosis in mice: abnormal myocardial response to freeze-thaw injury. Lab Anim Sci 40:616–619
4. Deguchi H (1981) Ultrastructural alterations of the myocardium in coxsackie B-3 virus myocarditis in mice: 18-month follow-up study by transmission and analytical electron microscopy. Jpn Circ J 45:695–712
5. Deguchi H, Kitaura Y, Morita H, Kotaka M, Kawamura K (1985) Cell-mediated in coxsackie B3 virus myocarditis in mice: in situ characterization by monoclonal antibody of mononuclear cell infiltrates. Heart Vessels [Suppl 1]:221–227
6. DiPaolo JA, Strong LC, Moore GE (1964) Calcareous pericarditis in mice of several genetically related strains. Proc Soc Exp Biol Med 115:496–497
7. Eaton GJ, Custer RP, Johnson FN, Stabenow KT (1978) Dystrophic cardiac calcinosis in mice: Genetic, hormonal, and dietary influences. Am J Pathol 90:173–186
8. Ewald R Weibel (ed) (1979) Stereological methods: practical methods for biological morphometry, vol 1. Academic Press London, pp 349–357
9. Fauci AS, Harley JB, Roberts WC, Ferrans VJ, Gralnick HR, Bjornson BH (1982) The idiopathic hypereosinophilic syndrome: clinical, pathophysiologic, and therapeutic considerations (NIH conference). Ann Intern Med 97:78–92
10. Hare WV, Stewart HL (1956) Chronic gastritis of the glandular stomach, adenomatous polyp of the duodenum, and calcareous pericarditis in strain DBA mice. J Natl Cancer Inst 16:889–912
11. Hayashi T, Okamoto F, Terasaki H, Deguchi H, Hirota Y, Kitaura Y, Spry CJF, Kawamura K (1996) Ultrastructural and immunohistochemical studies on myocardial biopsies from a patient with eosinophilic endomyocarditis. Cardiovasc Pathol 5: 105–112
12. Hirota Y (1994) Restrictive cardiomyopathy, cardiac amyloidosis, and hypereosinophilic heart disease. In: Abelmann WH (ed) Atlas of heart diseases. Cardiomyopathies, myocarditis, and pericardial disease. Current Medicine, Philadelphia, pp 5.1–5.15
13. Izumi T, Maisch B, Kochsiek K (1987) Experimental murine myocarditis after immunization with cardiac membranous protein. Eur Heart J 8 [Suppl J.]:419–424
14. Kawamura K, Kitaura Y, Morita H, Deguchi H, Kotaka M (1985) Viral and idiopathic myocarditis in Japan: a questionnaire survey. Heart Vessels [Suppl 1]:18–22
15. Kishimoto C, Spry CJF, Tai PC, Tomioka N, Kawai C (1986) The in vivo cardiotoxic effect of eosinophilic cationic protein in an animal preparation. Jpn Circ J 50:1264–1267
16. Kitaura Y (1981) Experimental coxsackie B virus myocarditis in mice: 18-month histopathological and virological study. Jpn Circ J 45:747–762
17. Kitaura Y, Morita H, Deguchi H, Kotaka M, Kawamura K (1984) Histopathologic and hemodynamic study of the heart in spontaneously developed perimyocarditis in DBA/2 mice (abstract). International Symposium on Cardiomyopathy and Myocarditis, Tokyo, Japan, 12–15 December. Heart Vessels [Suppl 1]:311
18. Kotaka M, Kitaura Y, Deguchi H, Kawamura K (1990) Experimental influenza A virus myocarditis in mice. Am J Pathol 136 2:409–419
19. Maeda N, Doi K, Mitsuoka T (1986) Development of heart and aortic lesions in DBA/2NCrj mice. Lab Anim 20:5–8
20. Matsumori A, Kawai C (1982) An animal model of congestive (dilated) cardiomyopathy: Dilatation and hypertrophy of the heart in the chronic stage in DBA/2 mice with myocarditis caused by encephalomyocarditis virus. Circulation 66 2: 355–360
21. Nabons CE, Ball CR (1969) Spontaneous calcification in hearts of DBA mice. Anat Rec 164:153–162
22. Nakayama Y, Kohriyama T, Yamamoto S, Deguchi H, Suwa M, Kino M, Hirota Y, Imamura K, Kitaura Y, Kawamura K, Spry CJ (1985) Electron-microscopic and immunohistochemical studies on endomyocardial biopsies from a patient with eosinophilic endomyocardial disease. Heart Vessels [Suppl 1]: 250–255
23. Noda S (1980) Histopathology of endomyocardial biopsies from patients with idiopathic cardiomyopathy. Quantitative evaluation based on multivariate statistical analysis. Jpn Circ J 44:95–116
24. Rings RW, Wagner JE (1972) Incidence of cardiac and other soft tissue mineralized lesions in DBA/2 mice. Lab Anim Sci 22:344–352
25. Spry CJF, Tai TC (1976) Studies on blood eosinophils. Clin Exp Immunol 24:423–434
26. Van-Vleet JF, Ferrans VJ (1987) Ultrastructural changes in inherited cardiac calcinosis of DBA/2 mice. Am J Vet Res 48: 255–261
27. Yamate J, Tajima M, Maruyama Y, Kudow S (1987) Observations on soft tissue calcification in DBA/2NCrj mice in comparison with CRJ:CD-1 mice. Lab Anim 21:289–298